



Review article

Modelling human control of steering for the design of advanced driver assistance systems



Franck Mars^{a,*}, Philippe Chevrel^b

^aUMR CNRS 6004, Laboratoire des Sciences du Numérique de Nantes (LS2N), CNRS & Centrale Nantes, 1, rue de la Noë - B.P. 92101, 44321 Nantes Cedex 03, France

^bUMR CNRS 6004, Laboratoire des Sciences du Numérique de Nantes (LS2N), IMT Atlantique, 4, rue Alfred Kastler - La Chantrerie, CS 20722, 44307 Nantes Cedex 03, France

ARTICLE INFO

Article history:

Received 15 July 2017

Revised 22 September 2017

Accepted 24 September 2017

Available online 5 October 2017

Keywords:

Cybernetic driver model

Haptic shared control

Human-machine cooperation

LQ preview

Robustness

Kalman filter

Online identification

Diagnosis

Distraction

ABSTRACT

This paper reviews a set of scientific studies on how driver modelling may serve as the basis for designing advanced driving assistance systems. The work was aimed at explicitly representing the human visual and motor processes involved in the control of steering, and took into account current knowledge in the behavioural sciences. The nature and structure of the model, and its calibration using experimental data (identification), were addressed. Two design applications were considered: 1) estimating the driver state in various conditions of distraction and 2) building an automatic controller for haptic shared control of the steering wheel.

© 2017 Elsevier Ltd. All rights reserved.

Contents

1. Introduction	293
2. A cybernetic driver model of steering control	293
2.1. Structure and foundations of the model	293
2.2. Cybernetic driver model identification	294
3. Model-based estimation of driver distraction	295
3.1. Detecting distraction through output or input disturbance estimation	296
3.2. Discriminating distraction types through parameter analysis	296
3.3. Conclusion	297
4. Haptic shared control of the steering wheel	297
4.1. Cooperation indicators for HSC	297
4.2. Synthesis of an electronic co-pilot for HSC	298
4.2.1. H2 preview	298
4.2.2. DVR model and control synthesis	299
4.2.3. Shared control with or without the driver model	299
4.3. Conclusion	300
5. General conclusion	300
Acknowledgements	300
Appendix. Detailed notations	300

* Corresponding author.

E-mail addresses: franck.mars@ls2n.fr (F. Mars), Philippe.Chevrel@imt-atlantique.fr (P. Chevrel).

A. Cybernetic driver model	300
B. Distraction and haptic shared control (HSC) indicators and variables	301
C. Vehicle-road model (VR)	301
References	302

1. Introduction

One of the key problems for the design of advanced driver assistance systems has been to predict the driver behaviour. The short-term prediction of the driver state, behaviour or intention could lead to the adaptation of a future interaction. For example, the prediction of a driver's action on the vehicle's commands at a given point in time may give warning of an imminent critical situation. Conversely, an assessment that could be judged as critical on the basis of the observation of the vehicle-road system alone could be assessed as non-critical if it was predicted that the driver was already engaged in a correction maneuver. To address this question, we incorporated a driver model into the design process of driver assistance systems.

We used an interdisciplinary approach that consists of the design of human-machine systems on the basis of a model that explicitly represents the human perceptual, motor and cognitive processes involved in the task. The driver model used is termed cybernetic in accordance with A. N. Kolmogorov's definition of cybernetics: "the study of systems of any nature which are capable of receiving, storing and processing information so as to use it for control." Our goal was indeed to understand, study and reproduce the human way of driving. This model and its application focuses specifically on steering control, although the same approach could be adapted for other types of human-machine dynamic interaction. Hence, the inspiration for the model was current knowledge of the psychology of perception and the neurophysiology of motor systems. It represents perceptually valid sensory cues used by drivers and neurophysiologically valid sensorimotor systems. The rationale behind such an approach was first to build a theoretically grounded model that may be relevant both for control theory and for human behavioural science. From a more practical point of view, it was also a way to orient design choices as a function of specific hypotheses on the nature of perceptual and motor systems.

The first section of the paper will present the model structure and its psychophysiological foundations. It will also briefly address the question of its identification. Then, we will present how it has been used to detect and discriminate various states of driver distraction using the model prediction error, an analysis of the parameter variations or by considering distraction as an input additive disturbance. Finally, the application of the model in the design of a haptic shared control (HSC) automaton will be presented to show how model prediction can help to improve steering performance and to propose innovative indicators for evaluating the quality of human-machine cooperation. In the appendix, notations relating to models, control and indicators are given.

2. A cybernetic driver model of steering control

2.1. Structure and foundations of the model

Many attempts have been made to model driver steering behaviour as a lateral deviation regulator on the track. The approaches used have included optimal control, fuzzy logic, and neural networks (Plöchl & Edelmann, 2007). The validity of these models is most often limited to specific driving situations, in which the driver acts as a control organ, determining the actions required

to follow the desired trajectory (Cacciabue, 2007). According to Mulder, Paassen, and Boer (2004), these models often ignore certain characteristics of human perception, which may affect control. Conversely, a cybernetic approach aims to represent the underlying psychological and physiological processes in accordance with current knowledge on sensorimotor control and cognition in humans. This is the approach we adopted in this study, whilst still maintaining our original aim to develop a simple enough model for use in the context of driving assistance design.

Fig. 1 presents the general architecture of the driver model. In order to steer the vehicle, the driver first needs to pick up relevant information from the visual scene (perception of the environment). Then, he must process this visual information to determine where he wants to drive. It has been proposed by Donges (1978) that the visual control of steering can be modelled as two complementary processes. One is fed by far visual information and allows for the anticipation of changes in the road curvature. The other is fed by near visual information and allows for the on-line correction of lateral position errors. This two-levels scheme has been validated by various experimental and modelling studies (Frissen & Mars, 2014; Land & Horwood, 1995; Salvucci & Gray, 2004). Visual information processing gives rise to a steering intention that needs to be converted by the neuromuscular systems into a force applied on the steering wheel, taking into account force and position feedback from the steering system.

The cybernetic model presented in Fig. 2 is consistent with the general architecture shown in Fig. 1. This model integrates and builds on previous work by our group (Sentouh, Chevrel, Mars, & Claveau, 2009) and that of others (Hoult & Cole, 2008; Salvucci & Gray, 2004). The reader can refer to Mars, Saleh, Chevrel, Claveau, and Lafay (2011) for details about the model theoretical background and to Saleh, Chevrel, Mars, Lafay, and Claveau (2011) for its implementation. The following section presents the essential points.

Visual anticipation is achieved by a simple proportional action on the angle at the tangent point, θ_{far} (Fig. 1). Land and Lee (1994) showed that drivers directed 65% of their glances toward the tangent point; thus, it has been proposed that looking at this point may be a way to read the road curvature at the sensorimotor level. Mars (2008) showed for instance that encouraging drivers to track any point that has the dynamics of the tangent point (but are not necessarily the tangent point itself) improves steering performance. However, it has also been debated that drivers may look at the future path (Wilkie, Kountouriotis, Merat, & Wann, 2010) or at the boundary of a safe trajectory envelope (Mars & Navarro, 2012), which often falls in the area of the tangent point. Whatever the case may be, we considered that using the tangent point as input to visual anticipation was a good enough approximation of visual information pickup in human drivers. In all cases, it more adequately represents information processing than solutions advocated in the past, which considered road geometry as a direct input to the driver model (Donges, 1978; Hess & Modjtahedzadeh, 1990).

It has been demonstrated that the visual compensation of lateral position errors can be achieved through peripheral vision of the road edge lines (Summala, Nieminen, & Punto, 1996). In line with a study by Salvucci and Gray (2004), we assumed that this can be represented as the compensation of the angular deviation of a near point (θ_{near}) perceived at a distance $\ell_s=5$ m from the front

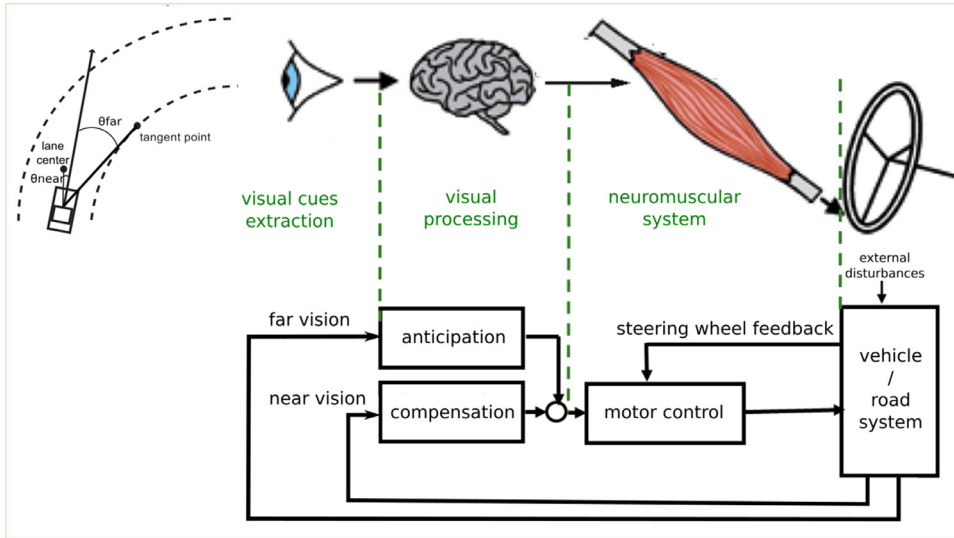


Fig. 1. General architecture of the driver model.

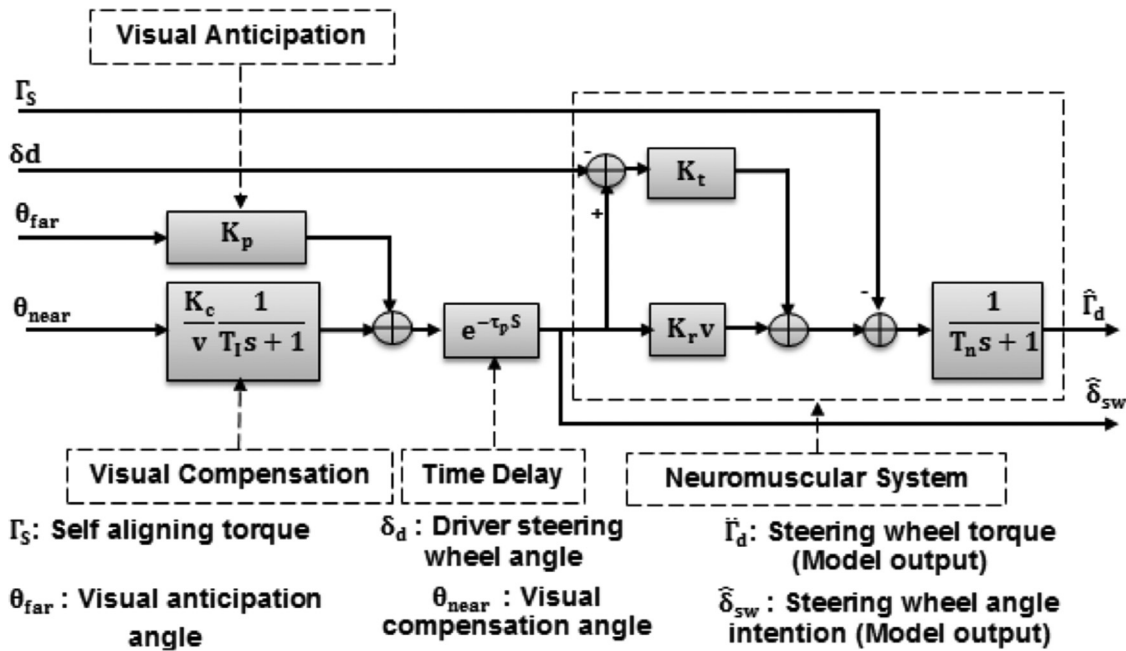


Fig. 2. The cybernetic driver model (Mars et al., 2011; Saleh et al 2011).

of the vehicle. In some respects, this transmittance (Fig. 2) represents the integration by the driver of the lateral dynamics of the vehicle. Visual anticipation and compensation were combined to generate an angle $\hat{\delta}_{sw}$, which is supposed to consist of the driver's intention in terms of steering wheel angle, taking into account the processing time τ_p . $\hat{\delta}_{sw}$ serves as input to the neuromuscular system.

The model of the neuromuscular system is based on work by Houtl and Cole (2008). Like its inspiration, our model reproduces the principle of muscle co-activation through α - and γ -motoneuron signals, which can be considered as feedforward and feedback control of movement execution (see Mars, et al., 2011 for more details). Unlike Houtl and Cole (2008), however, the model output is torque on the steering wheel, ($\hat{\Gamma}_d$), not an angle. This property is more realistic and also consistent with the objective of developing a haptic shared-control system that complements the force applied on the steering wheel by the driver (see Section 4). The neuromuscular system is defined by three parameters. The

gain K_t represents the motor reflex that verifies the actual steering wheel angle δ_d conforms to the desired angle $\hat{\delta}_{sw}$; it does so to compensate for any external perturbations (e.g., roadway conditions or gusts of wind). The gain K_r represents the internal model of steering stiffness. It is multiplied by the speed of the vehicle to take into account the fact that steering stiffness increases with speed. Arm dynamics were modelled by a first-order transmittance. At the input of the neuromuscular subsystem, the torque Γ_s accounts for the steering wheel force feedback, as perceived by the driver. Such haptic feedback improves the driver's perception and contributes to the stabilization of the vehicle.

2.2. Cybernetic driver model identification

The cybernetic model was identified from experimental data that was obtained using forward-facing cameras and steering wheel measures. The parameter vector was estimated first by

Saleh et al. (2011), and revisited later (Ameyoe, Mars, Chevrel, Le Carpentier, & Illy, 2015; Hermannstädter & Yang, 2013), using constrained prediction error identification (PEM, Ljung, 1999). The state-space structured linear representation of the driver model is:

$$\begin{cases} \dot{x}_d(t) = A(\theta)x_d(t) + B(\theta)u(t) \\ y(t) = C(\theta)x_d(t) + D(\theta)u(t) \end{cases} \quad (1)$$

with $x_d = [x_{d1} \ x_{d2} \ x_{d3}]^T$ the state vector, $u = [\theta_{far} \ \theta_{near} \ \delta_d \ \Gamma_s]^T$ and $y = [\hat{\Gamma}_d \ \delta_{sw}]^T$ are the inputs and outputs vectors. The model parameters that have to be identified are stored in the parameter vector $\theta = [K_p \ K_c \ T_I \ \tau_p \ K_r \ K_t \ T_n]$. The continuous state-space matrices corresponding to Eq. (1) are:

$$A(\theta) = \begin{bmatrix} -\frac{1}{T_I} & 0 & 0 \\ \frac{2}{\tau_p} & -\frac{2}{\tau_p} & 0 \\ -\frac{(K_r V + K_t)}{T_n} & 2\frac{(K_r V + K_t)}{T_n} & -\frac{1}{T_n} \end{bmatrix},$$

$$B(\theta) = \begin{bmatrix} 0 & \frac{K_c}{V T_I} & 0 & 0 \\ 2\frac{K_p}{\tau_p} & 0 & 0 & 0 \\ 0 & 0 & -\frac{K_t}{T_n} & -\frac{1}{T_n} \end{bmatrix}$$

$$C(\theta) = \begin{bmatrix} 0 & 0 & 1 \\ -1 & 2 & 0 \end{bmatrix} \text{ and } D(\theta) = \begin{bmatrix} 0 & 0 & 0 & 0 \\ -K_p & 0 & 0 & 0 \end{bmatrix}$$

In Saleh et al. (2011) and Hermannstädter and Yang (2013), off-line identification was performed to estimate the parameter vector. This considered the output prediction error signal¹ power as the criterion that needed to be minimized. The Gauss-Newton search-scheme was used to solve the nonlinear optimization problem, assuming local identifiability, and considering starting values and interval constraints given in Saley et al. (2011). Saley et al. (2011) first showed that the model could be successfully identified for five different drivers. The identification procedure converged to the same range of values in all cases. A validation test was also carried out to confirm that the model could successfully steer itself along a road and show behaviour that was close to that of human drivers. In this test, the model was implemented in a driving simulator and the results compared with those of the human driver who provided data for identification. The results show that the driver and the identified model exhibited very similar trajectories. Hermannstädter and Yang (2013) performed successful identification on a set of 14 drivers, using an instrumented vehicle on real roads. Finally, in a driving simulator study that involved 35 participants, Ameyoe, Chevrel, Le Carpentier, Mars, and Illy (2015) reported that the fit ratio between the model prediction and the experimental data was above 90% for all drivers, at least when they were not distracted by a secondary task.

In a study by Ameyoe, Chevrel, et al. (2015), the problem was considered as a nonlinear observation problem and solved recursively using unscented Kalman filtering (UKF). The advantage of this approach was being able to acquire continuous information on the evolution of the model parameters over time. The parameter vector that need to be identified is assumed to be time varying, with stochastic properties borrowed from a Wiener process. The state space equations of both the cybernetic model and the Wiener process used to model the parameter vector were then discretized and concatenated in a single non-linear state-space model. In the next stage, the state of this augmented model was estimated using observer theory. The results obtained with UKF were as good as those from using the PEM method.

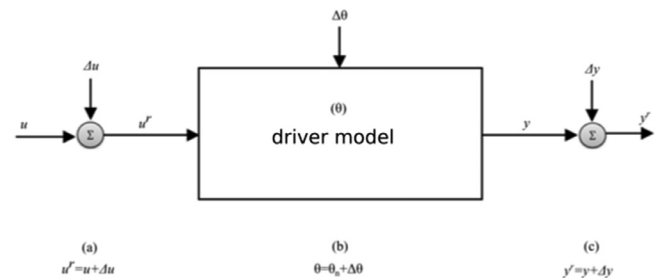


Fig. 3. Three ways of considering the effect of distraction on the driver model: (a) input disturbance, (b) parametric disturbance, (c) output disturbance.

Table 1
Cybernetic driver model parameters.

Parameters	Description
K_p	Visual anticipation gain
K_c	Visual compensation gain
T_I	Visual compensation time constant
τ_p	Processing delay
K_r	Gain of the internal model of steering compliance
K_t	Gain of the stretch reflex
T_n	Neuromuscular time constant
V	Vehicle speed

3. Model-based estimation of driver distraction

Distraction contributes to a significant number of road fatalities; thus, a great deal of work has already been conducted to design an algorithm for the diagnosis of the driver distractive state. This has been mainly achieved through the analysis of the driver's gaze, steering behaviour and psychophysiological indicators (Dong, Hu, Uchimura, & Murayama, 2011; Nakayama, Futami, Nakamura, & Boer, 1999; Yang, McDonald, & Zheng, 2012). Recently, some effort has also been made to base the diagnosis on a driver model through a parameter analysis or by analyzing the model prediction error. Ameyoe, Mars, et al. (2015) and Hermannstädter and Yang (2013), adopted this approach. The goal was to create indicators that help to detect distraction without the direct video monitoring of drivers, and possibly to discriminate the exact nature of that distraction.

Assuming that distraction affects vehicular control, particularly steering control, our study's main motivation was to consider distraction as disturbances or uncertainties affecting the cybernetic model. This is illustrated in Fig. 3 by considering three different assumptions:

- Distraction affects driver perception through the input disturbance Δu ;
- Distraction affects drivers in a way that impacts one or several model parameters more than others, depending on the type of distraction; in this case, distraction is considered as multiplicative disturbances, $\Delta\theta$, affecting specific model parameters (see Table 1)
- Distraction directly affects the torque applied by the driver on the steering wheel; this can be considered as an additive disturbance Δy of the output of the cybernetic model.

The various proposed methods to assess and categorize driver distraction rely on the analysis of signals or parameter values obtained after the identification of the cybernetic driver model. To achieve this goal, we performed an experiment using a driving simulator. Thirty-five participants participated in the experiment. For each trial, the participants drove around an experimental track that consisted of 20 bends separated by sections of straight road. The protocol interleaved periods of baseline driving (no distraction) with periods of distracted driving. Four types of distraction

¹ The difference between the observed driver steering torque and the torque that was predicted by the driver model.

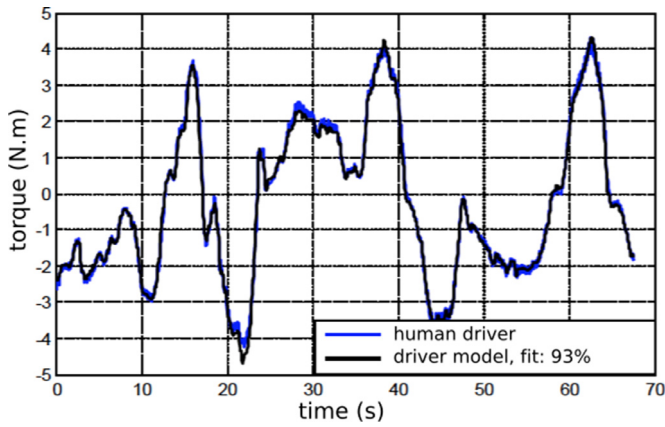


Fig. 4. Comparison between observed and predicted torque during undistracted driving for 70 s of driving data. Reproduced from Ameyoe, Chevrel, et al. (2015).

were tested: cognitive (backward counting task), visual (reading a peripheral text), visuomotor (dialing task with mandatory visual control) and motor (dialing whilst looking at the road). A supplementary condition was added to assess the influence of driving with one hand without a secondary task. Partial results have been presented before. They focused on disturbance estimation (Ameyoe, Mars, et al., 2015) or parameter analysis (Ameyoe, 2016; Mars, Ameyoe, Chevrel, Carpentier, & Illy, 2017). They will be reviewed together here for the first time. The reader should refer to Ameyoe, Mars, et al. (2015) for a complete methodological description of the experiment.

3.1. Detecting distraction through output or input disturbance estimation

Ameyoe, Mars, et al. (2015) showed that the cybernetic driver model proposed by Mars et al. (2011) and Saleh, Chevrel, Mars, Lafay, and Claveau (2011), was able to predict human driver steering behaviour with a good accuracy in normal driving conditions. For all participants, the fit ratio between the model prediction and the experimental data was above 90%. Fig. 4 is an individual illustration of that ability.

One way to detect distraction is to consider the difference between the model output and the observed steering behaviour as the consequence of distraction (Fig. 3c). This was the approach used in Ameyoe, Mars, et al. (2015). The authors proposed a new indicator, the Torque Prediction Indicator (TPI), which is the signal power of the difference between the observed driver steering torque and the torque predicted by the driver model during the considered period. It was computed as follows:

$$TPI = \left(\frac{1}{T_w} \int_0^{T_w} (\Gamma_d(t) - \hat{\Gamma}_d(t))^2 dt \right)^{\frac{1}{2}}$$

with:

- T_w (s): length of the observation window, results were obtained with $T_w = 70$,
- Γ_d (N m): driver torque,
- $\hat{\Gamma}_d$ (N m): predicted torque.

The results showed that the effects observed on the TPI were in large part consistent with the steering performance indicators, especially lateral position variability. The TPI was particularly sensitive to visuomotor distraction (Fig. 5), which also yielded the larger steering impairment. Visual and motor distraction also influenced the TPI, although the effect did not reach statistical significance for

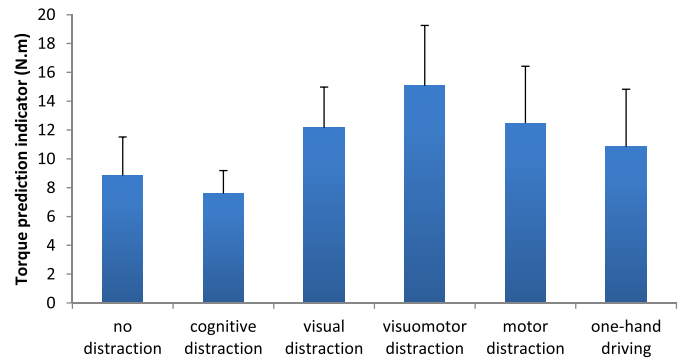


Fig. 5. The torque prediction indicator averaged across participants as a function of driving conditions. Error bars represent the standard error of the mean.

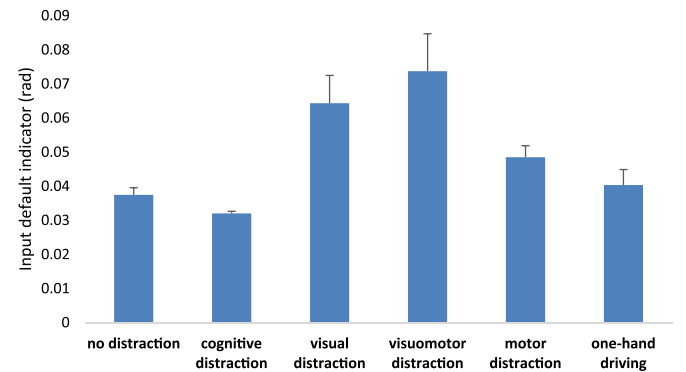


Fig. 6. The input default indicator averaged across participants as a function of driving conditions. Error bars represent the standard error of the mean.

the motor distraction. Those results constituted a first step in validating the sensitivity of the driver model to driver distraction. The TPI may be considered as an alternative to steering performance indicators, such as the lateral position variability or the steering reversal rate.

Ameyoe (2016) also attempted to explain distraction by assuming that the visual or visuomotor distraction affected the visual input of the driver model. In this case, distraction is regarded as an additive input disturbance (Fig. 3a), which is considered as a stochastic signal. A second order dynamic model was used to encapsulate the main characteristics of this virtual signal. Once concatenated with the driver model, the resulting model served as a support for the observer, capable of estimating the continuous disturbance signal. This method used an ad-hoc Kalman filter to estimate the disturbance signal of the visual compensation input. Experimental data obtained from the driving simulator was used. An input default indicator (IDI) was computed as follows:

$$IDI = \left(\frac{1}{T_w} \int_0^{T_w} \Delta u(t)^2 dt \right)^{\frac{1}{2}}$$

with:

- T_w (s): length of the observation window, results were obtained with $T_w = 70$,
- Δu (rad): additive disturbance on the visual compensation input of the driver model.

The results showed that it was indeed specifically sensitive to visual and visuomotor distraction (Fig. 6).

3.2. Discriminating distraction types through parameter analysis

Another way to approach distraction estimation is to categorize driver distraction on the basis of the analysis of the cybernetic

Table 2

Sensitivity of performance indicators and model parameters to the different types of distraction; sensitive (+) versus non-sensitive (–).

Distraction type	Steering performance		Parameter analysis			
	SDLP	SWRR	K_p	K_c	K_t	T_n
Cognitive	–	–	–	–	–	–
Motor	+	+	–	–	–	+
Visual	+	+	–	+	+	+
Visuomotor	+	+	+	+	+	+

driver model parameters (Fig. 4b). As the model parameters represent visual and motor processes that determine steering behaviour, it can be hypothesized that some of them may be selectively sensitive to some types of distraction. For this reason, Hermanstater and Yang (2013) performed an online identification, dealing iteratively with packets of input-output data measured on an experimental car. Driving without distraction was compared with driving with visual and auditory distraction. The results revealed that the two visual parameters, i.e., K_p for anticipation and K_c for compensation, were selectively influenced by visual distraction. The same approach was applied to the data gathered from the driving simulator experiment presented earlier, which compared visual, motor, visuomotor and cognitive distractions. Four selected driver model parameters were identified: K_p and K_c , but also K_t and T_n for the neuromuscular system.

The results are summarized in Table 2. Cognitive distraction did not significantly influence the steering performance indicators, i.e., the standard deviation of lateral position (SDLP) and the steering wheel reversal rate (SWRR). Accordingly, no parameter variation was observed. Conversely, SDLP and SWRR increased with motor, visual and visuomotor distraction. It was not possible to discriminate between these different types of distraction on the basis of driving performance alone. In this respect, the parameter values were more useful. Motor distraction only influenced the arm dynamics time constant T_n . Visual distraction also influenced T_n , together with K_t , the gain of motor correction reflex, and K_c , the gain of visual compensation. Visuomotor distraction showed very similar effects on these three parameters. It was also the only condition that brought about a decrease in the gain of visual anticipation, K_p , most probably because the visuomotor task was much more demanding on the visual system (gaze was directed to the side and downward) than the visual task (gaze was directed to the side only). This suggests that K_p is quite robust, except in extreme cases of distraction. Taken together, the results suggest that the driver model parameters are sensitive to the driver state of distraction; indeed, they varied as a function of the secondary task. More work is needed now to build a robust estimator of distraction using on-line parameter analysis.

3.3. Conclusion

The rationale for this work was that distraction can be categorized as cognitive, visual or motor, and that each type of distraction has a different influence on steering behaviour. So, the question is: can a visuomotor model help to detect and discriminate distraction episodes? The method consisted first in parameter identification during a training period without distraction. Then, on-line parameter identification or disturbances estimation was performed when distraction occurred. The results showed that scrutinizing how the values of the parameters evolve makes it possible to discriminate between cognitive, visual and motor distraction, at least to some extent. The advantage of modelling distraction using an additive output disturbance on the driver model obtained in normal condition (no distraction) is that robust filtering is required rather than on-line identification. However, although distraction could be de-

tected, it was not really possible to discriminate between different types of distraction. Lastly, modelling the distraction as additive input disturbances should make possible some sort of discrimination, assuming that distractions with a visual component would mainly affect signals associated with visual perception. However, more work is needed to confirm this assumption.

4. Haptic shared control of the steering wheel

The second way our driver model has been used for driving assistance system design relates to haptic shared control (HSC) of the steering wheel. Some of this work has been presented in Saleh, Chevrel, and Lafay (2012) and Saleh, Chevrel, Claveau, Lafay, and Mars (2012, 2013). It will be summarized and complemented in the following section.

HSC occurs when a driver and an automaton continuously and simultaneously act on the steering wheel to achieve lateral control. It has been demonstrated to facilitate steering control whilst keeping the driver in the loop (Abbink, Mulder, & Boer, 2012; Mulder, Abbink, & Boer, 2012; Sentouh, Soualmi, Popieul, & Debernard, 2013; Wang, Zheng, Kaizuka, Shimono, & Nakano, 2017). Like a traditional lane-keeping system, it has a direct influence on the vehicle's trajectory. At the same time, it provides haptic guidance to the driver, improving comfort and workload (Mars, Deroo, & Charon, 2014; Mars, Deroo, & Hoc, 2014). The benefit is that the driver is aware of the system's actions, and can choose to overrule them.

Lane-keeping systems are often designed on the basis of a vehicle-road model and consider driver action as a disturbing signal. Thus, these systems do not guarantee global stability and cannot provide a robustness analysis when variations in driver behaviour occur. A performance analysis of lane-keeping systems has highlighted the fact that, together, a vehicle and its driver form a human-machine system. Such a system should be considered as a whole in order to develop a cooperative co-pilot that monitors the driver's control actions, and understands and corrects them if necessary. For this reason, a cybernetic approach is recommended for modelling any interactions between the driver and the vehicle-environment system (Mulder et al., 2004).

Saleh, Chevrel, Claveau, et al. (2012, 2013) sought to design and evaluate a HSC system based on the cybernetic driver model. The cybernetic driver model and the road-vehicle model were aggregated into the control synthesis model, known as the DVR model (see Section 4.2.2). The benefits of using the driver model will now be highlighted.

4.1. Cooperation indicators for HSC

The evaluation of control quality usually involves a tradeoff between multiple, potentially conflicting criteria. Steering assistance systems should assist the driver in keeping the vehicle within the lane, and thus contribute to active safety. At the same time, these systems should cooperate with the driver and avoid conflict as much as possible. In the absence of standards to evaluate the quality of HSC, Saleh, Chevrel, Claveau, et al. (2012, 2013) defined different indicators to enable the measurement of what is seen as "safe driving" and a "cooperative copilot". Some of these metrics are commonly used to measure lane-keeping performance, whilst others are innovative.

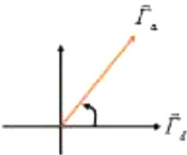
One of the most common metrics for lane-position performance evaluation is lateral deviation error. In particular, we chose to examine the mean absolute lateral deviation from the centre line and the standard deviation of lateral position. These indicators do not allow the evaluation of the lane-departure risk. Such risk can be measured, however, by using the time to lane crossing (TLC), defined as the time available to a driver until any part of the vehicle reaches one of the lane boundaries

(Godthelp, Milgram, & Blaauw, 1984). There are several ways of computing TLC values with more or less approximation of the road curvature and trajectory prediction (Mammar, Glaser, & Netto, 2006). Here, the TLC, or TLCP (for TLC Path), was estimated by assuming that the vehicle yaw rate and heading speed would remain constant in the near future. The advantage of TLCP is that it is less sensitive to transient steering deviations, because they are filtered by the vehicle dynamics.

The risk of lane departure is also driver-dependent; thus, TLCP alone cannot provide a consistent evaluation, especially when the driver intentionally cuts bends or when he is aware of the risk and has already acted to correct it. In these two cases, TLCP overestimates the risk, as it does not take into account the driver's intention. To overcome this deficiency, Saleh, Chevrel, Claveau, et al. (2012) suggested that the cybernetic model be used to estimate the driver's steering intention (see Fig. 2). The driving error (Δ_δ) is then defined as the deviation of the actual driver steering angle, δ_d , from the angle predicted by the driver reference model δ_{sw} . Finally, the Lane Departure Risk (LDR) criterion, $LDR = \Delta_\delta / TLCP$, was proposed as a mean of evaluating the risk of lane departure. The LDR value is normalized within a [0–1] risk interval. As long as LDR indicates a low threat level, driving is "safe".

On the other hand, new indicators of cooperation between the driver and the assistance system were proposed for the first time in Saleh, Chevrel, Claveau, et al. (2012):

- Consistency rate T_{co} : defined as the ratio of the period during which the assistance torque (Γ_a) is in the same direction as driver torque (Γ_d), divided by the total driving period.
- Resistance rate T_{res} : defined as the ratio of the period during which Γ_a is in the opposite direction to Γ_d but Γ_a is inferior to Γ_d , divided by the total driving period.
- Contradiction rate T_{cont} : defined as the ratio of the period during which Γ_a overcomes Γ_d , divided by the total driving period.
- Contradiction level P_c (Saleh, Chevrel, & Lafay, 2012), defined as the cosine of the angle between the torques Γ_d and Γ_a applied on the steering column respectively by the driver and the assistance device. These pairs constitute two signals of the Hilbert space whose norm and scalar product can be calculated.

$$P_c = \cos(\vec{\Gamma}_a, \vec{\Gamma}_d) = \frac{\int_0^{T_i} \Gamma_a(t) \times \Gamma_d(t) dt}{\sqrt{\int_0^{T_i} \Gamma_a^2(t) dt \times \int_0^{T_i} \Gamma_d^2(t) dt}}$$


P_c is equal to -1 if the assistance always exerts an opposite action to that of the driver (180° between the assistance torque and the driver torque). P_c is equal to 1 when the assistance systematically accompanies the driver (0°). More generally, P_c represents a good indicator of the agreement between the driver's action and that of the automated device.

4.2. Synthesis of an electronic co-pilot for HSC

4.2.1. H2 preview

The assistance strategy developed and evaluated by Saleh, Chevrel, Claveau, et al. (2012) and Saleh, Chevrel, Claveau, Lafay, and Mars (2013), used LQ/H2-Preview control theory (Saleh, Chevrel, & Lafay, 2012) applied to the global DVR model. Such a control design is known to guarantee improved performance when the near future of the exogenous signal, in this case the road curvature ρ_{ref} , is known (preview). Moreover, the authors revealed that the LQ criterion can potentially take the indicators

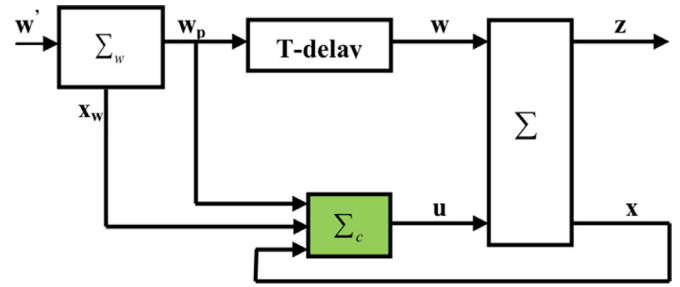


Fig. 7. H2-Preview controller problem.

of cooperation quality into account. Let's first recall the general result.

In Fig. 7, the process model Σ is defined through Eq. (2), the exogenous signal model Σ_w is defined by Eq. (3), and the controller Σ_c is synthesized.

$$\begin{aligned} \dot{x} &= Ax + B_1 u + B_2 w \\ z &= Cx + D_1 u \\ A &\in \mathbb{R}^{n \times n}, B_1 \in \mathbb{R}^{n \times m}, B_2 \in \mathbb{R}^{n \times r}, C \in \mathbb{R}^{p \times n}, D_1 \in \mathbb{R}^{p \times m} \end{aligned} \quad (2)$$

x , u , w and z above respectively denote the state vector, the control input, the disturbance input and the performance vector output. The disturbance input w is assumed to be previewed the over time horizon T . So, $w_p(t) = w(t+T)$ is an input of the controller. Moreover, this signal is supposed to be a coloured noise obtained by filtering the white noise w' through Σ_w (see Eq. (3)).

$$\begin{aligned} \dot{x}_w &= A_w x_w + B_w w' \\ w_p &= C_w x_w \\ A_w &\in \mathbb{R}^{q \times q}, C_w \in \mathbb{R}^{r \times q}, B_w \in \mathbb{R}^{q \times r} \end{aligned} \quad (3)$$

The "optimal H2 preview controller problem" (Marro & Zattoni, 2005) is defined as the problem of finding a controller Σ_c that rejects the effect of the input disturbance w (known in advance over the time T) on the output z . More precisely, the controller Σ_c has to minimize the H2 performance index (6) whilst stabilizing the closed-loop system (Fig. 7). The general solution to this problem is recalled in Theorem 1.

$$J = \|z\|_2^2 = \int_0^\infty z^T(t)z(t)dt \quad (4)$$

Theorem 1. let the system (Σ, Σ_w) be defined by (2) and (3). Assume that:

- the pair (A, B_1) is stabilizable
- the quadruple (A, B_1, C, D_1) has no invariant zeros on $i\mathbb{R}$
- D_1 is full-column rank matrix
- A_w is Hurwitz

Let $R = D_1^T D_1$, $Q = C^T C$, $S = C^T D_1$, then, the solution of the H2-preview problem is given by the controller Σ_c defined through the following equation:

$$u(t) = -K_+ x(t) + \int_0^T \Phi(\tau) w_p(t - \tau) d\tau - R^{-1} B_1^T e^{A_+^T (T - \tau)} M x_w(t) \quad (5)$$

where :

- $K_+ = R^{-1}(S^T + B_1^T P_+)$ is the gain feedback matrix
- $\Phi(\tau) = -R^{-1} B_1^T e^{A_+^T (T - \tau)} P_+ B_2$,
- P_+ is the stabilizing solution of the algebraic Riccati equation : $PA + A^T P - (S + PB_1)R^{-1}(S^T + B_1^T P) + Q = 0$
- $A_+ = A - BR^{-1}(S^T + B^T P_+)$ is the closed loop matrix

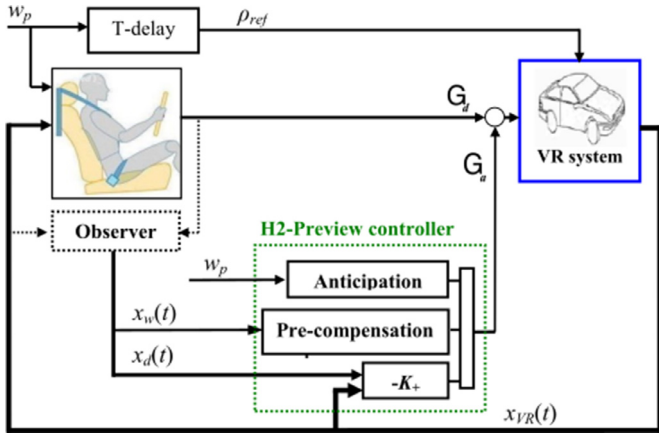


Fig. 8. H2-Preview shared control.

$$z = Q_z^{1/2} \begin{bmatrix} \psi_L \\ y_{act} \\ a \\ \Gamma_a - \alpha \Gamma_d \\ \Gamma_d \\ \Gamma_a \end{bmatrix} \quad \text{where :}$$

$$Q_z = \begin{bmatrix} c_1 & 0 & 0 & 0 & 0 & 0 \\ 0 & c_2 & 0 & 0 & 0 & 0 \\ 0 & 0 & c_3 & 0 & 0 & 0 \\ 0 & 0 & 0 & c_4 & 0 & 0 \\ 0 & 0 & 0 & 0 & c_5 & c_{da} \\ 0 & 0 & 0 & 0 & 0 & 1 \end{bmatrix} \quad (7)$$

with:

With this, the criterion (4) is equivalent to:

$$J = \|z\|_2^2 = c_1 \|\psi_L\|_2^2 + c_2 \|y_{act}\|_2^2 + c_3 \|a\|_2^2 + c_4 \|\Gamma_a - \alpha \Gamma_d\|_2^2 + c_5 \|\Gamma_d\|_2^2 + \|\Gamma_a\|_2^2 + c_{da} \int_0^{+\infty} \Gamma_d(\tau) \times \Gamma_a(\tau) d\tau \quad (8)$$

o M is the solution of the Sylvester equation :

$$A_+^T M + M \cdot A_w + P_+ B_2 C_w = 0$$

For the proof, see Saleh, Chevrel, and Lafay (2012).

Based on this result, the synthesis of the assistance controller was performed in continuous time to minimize the H2 performance index with the performance vector z (see next section) containing signals correlated with road tracking quality (ex. heading angle error ψ_L), lane keeping quality (ex. lateral deviation y_L), control effort (assistance torque Γ_a), driver-assistance sharing and co-operation quality ($\Gamma_a - \Gamma_d$ and the scalar product $\langle \Gamma_a, \Gamma_d \rangle$ whose value depends on the cosine of the angle between the two torques; see Section 4.1). In Saleh, Chevrel, and Lafay (2012), the road curvature was assumed to be coloured noise, with a zero mean value and a bandwidth restricted to the frequency interval $[0-20]$ rad/s. This is compatible with the signal model used and is incorporated into the H2 standard model that supports the H2 control synthesis.

Finally, the optimal preview shared control obtained consists of three terms (Fig. 8):

- A state-feedback term ($-K_+x$),
- An anticipation term elaborated through a finite impulse response filter (FIR) from the previewed curvature signal ($w_p(t) = \rho_{ref}(t+T)$) on the preview horizon T ,
- A pre-compensation term, which deals with the predicted road curvature beyond the preview horizon.

4.2.2. DVR model and control synthesis

The state-space DVR model, which aggregates the cybernetic driver model and the road-vehicle model has the following form, with ρ_{ref} the current road curvature:

$$\begin{bmatrix} \dot{\beta} \\ \dot{r} \\ \dot{\psi}_L \\ \dot{y}_L \\ \dot{\delta}_d \\ \dot{\delta}_d \\ \dot{x}_{1d} \\ \dot{x}_{2d} \\ \dot{\Gamma}_d \end{bmatrix} = \begin{bmatrix} a_{11c} & a_{12c} & 0 & 0 & a_{15c} & 0 & 0 & 0 & 0 & 0 \\ a_{21c} & a_{22c} & 0 & 0 & a_{25c} & 0 & 0 & 0 & 0 & 0 \\ 0 & 1 & 0 & 0 & 0 & 0 & 0 & 0 & 0 & 0 \\ V_x & l_s & V_x & 0 & 0 & 0 & 0 & 0 & 0 & 0 \\ 0 & 0 & 0 & 0 & 0 & 1 & 0 & 0 & 0 & 0 \\ a_{61c} & a_{62c} & 0 & 0 & a_{65c} & a_{66c} & 0 & 0 & b_{61c} & 0 \\ 0 & 0 & b_{12d} & b_{12d}/l_s & 0 & 0 & a_{11d} & 0 & 0 & 0 \\ 0 & 0 & b_{22d} & b_{22d}/l_s & 0 & 0 & a_{21d} & a_{22d} & 0 & 0 \\ b_{n31d} & b_{n32d} & b_{32d} & b_{32d}/l_s & b_{n35d} & 0 & a_{31d} & a_{32d} & a_{33d} & 0 \end{bmatrix} \begin{bmatrix} \beta \\ r \\ \psi_L \\ y_L \\ \delta_d \\ \delta_d \\ x_{1d} \\ x_{2d} \\ \Gamma_d \end{bmatrix} + \begin{bmatrix} 0 \\ 0 \\ 0 \\ 0 \\ 0 \\ b_{61c} \\ 0 \\ 0 \\ 0 \\ -b_{34d} \end{bmatrix} \Gamma_a + \begin{bmatrix} 0 \\ 0 \\ -V_x \\ -V_x l_s \\ 0 \\ 0 \\ 0 \\ b_{21d} D_{far} \\ b_{31d} D_{far} \end{bmatrix} \cdot \rho_{ref} \quad (6)$$

The H2 output performance vector z is defined from the output equation (see Eq. (9) in appendix) as:

The compromise between these different quantities is obtained by means of penalties on each signal, defined within the matrix Q_z . The penalty on the assistance torque Γ_a is set arbitrarily to 1 for standardization purposes. The others are adjusted according to the objectives pursued (the final choice of penalties: $c_1 = 200$, $c_2 = 20$, $c_3 = 3$, $c_4 = 5$, $c_5 = 1$, $c_{da} = -10$). The actions carried out in real time by the electronic co-pilot can be deduced directly from the resolution of the H2 preview synthesis problem (see Theorem 1). The assistance torque is thus modulated according to the compromise to be made between the risk of Lane Departure Risk (LDR) and the collaborative quality between the driver and the assistance device. For example, c_2 penalizes the lateral deviation, $\alpha \approx \Gamma_a/\Gamma_d$ informs about the desired level of sharing, with two specific cases: $\alpha \approx 0$ for manual driving, $\alpha = 1$ when steering is shared equally between the assistance device and the driver, and $\alpha \gg 1$ for fully automated driving; likewise, c_{da} negatively penalizes the scalar product between Γ_a and Γ_d , which prevents contradictory control between the driver and the assistance device (see contradiction level P_c defined above).

4.2.3. Shared control with or without the driver model

Saleh, Chevrel, Claveau, et al. (2012) compared two driving sessions with two types of shared control controllers. Both were based on the H2 preview scheme described above and both exploited the road curvature preview. The first controller optimized performance and safety criteria only (i.e., heading error, lateral deviation from the centreline, lateral acceleration and steering wheel torque). The other was based on the DVR model, which enabled additional cooperation criteria for optimization to be taken into account, i.e., $\alpha \approx \Gamma_a/\Gamma_d$ and the scalar product between Γ_a and Γ_d . The main results obtained with a level of sharing of 50% are

illustrated in Fig. 9.

In both cases, the level of lane keeping performance was good. Without HSC, the driver applied a cumulative torque of about

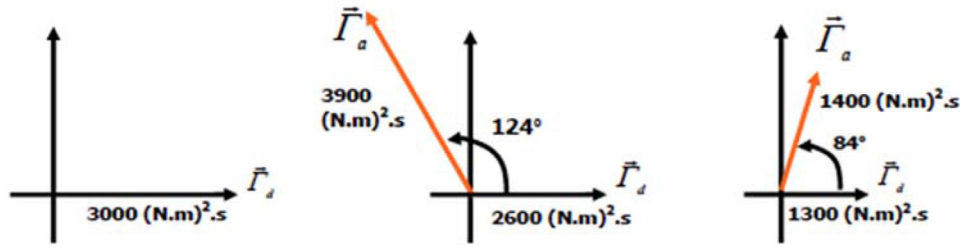


Fig. 9. Contradiction level between the driver torque Γ_d and the assistance torque Γ_a . From left to right: i) without HSC (driver=100%), ii) HSC without a driver model, iii) HSC with a driver model.

3000 (N m)² s (Fig. 9, left). With HSC without a driver model, the driver torque was reduced to 2600 (N m)² s, combined with a system torque of 3900 (N m)² s. However, the actions of the two agents were in large part in opposing directions, which translates as an angle above 90° between the two vectors (Fig. 9, centre). HSC with a driver model lead to a much larger agreement between the driver and the assistance device (angle below 90°). The torque applied by the driver on the steering wheel was reduced to 1300 (N m)² s, whereas the system delivered 1400 (N m)² s. In this case, the driver delivered 48% of the total torque, which is close to the targeted 50%.

4.3. Conclusion

This section highlights the importance of the cybernetic model for HSC, in particular: i) to make possible the definition of cooperation criteria for analysis and control synthesis, and ii) as support for robustness analysis (through μ -analysis), using parametric uncertainties to describe the diversity of human behaviour in steering (Saleh et al., 2013).

5. General conclusion

This paper reviewed the importance of a cybernetic driver model by considering two case-studies: driver distraction state estimation and HSC of the steering wheel.

First, the cybernetic model was presented and its psychological significance explained. The calibration of its parameters from real experiments was also discussed, considering either packet-based or recursive identification. Our experience is that such an identification is possible when driver torque can be correctly estimated. This led to the creation of a driver model that was able to steer our driving simulator by itself on various roads.

Second, we studied distraction modelling using additive or multiplicative disturbances on the non-distracted driver model. Our experience was that it provides new residues, which can be invaluable in detecting distraction, in some cases even distinguishing in some cases between types of distraction (e.g., visual, visuomotor and motor distraction). Based on this approach, some patents were deposited, illustrating its industrial relevance (Ameyoe, Illy & Chevrel et al. (2016); Illy, Ameyoe & Chevrel et al. (2017)).

Third, we considered HSC, with a design process based on the cybernetic driver model. We saw early on the importance of using such a driver model for shared control design (Mars et al., 2011, Saleh et al 2011). This was confirmed by Saleh, Chevrel, Claveau et al. (2012) and Saleh et al. (2013). Designing shared control with a driver-vehicle-road model enables a much more acceptable and robust solution to be found, with a wider application range. In addition, new indicators of cooperation quality that take into account short-term prediction of the driver action were defined. Such indicators were lacking in the literature. They may be a useful contribution for researchers who want to go beyond the traditional performance metrics to evaluate HSC systems.

The prediction capabilities offered by the cybernetic driver model were essential in the systems' design. For HSC, the driver model improves the stability of the global system by minimizing the risk of negative interferences that may occur in the near future between the human and the automaton, such as contradictory actions. For distraction estimation, the contribution of the model is not about predicting the interaction to come. Rather, it is about detecting early distraction and discriminating between different types of distraction on the basis of the difference between current actions and model predictions.

Future work based on the cybernetic driver model should consider more in-depth investigation of human driving and system acceptance, particularly in the context of the development of autonomous vehicles. It should also consider the central question of understanding how drivers adapt their behaviour to assistance devices. Individual tuning of the model parameters to each driver may offer a way to significantly improve the performance of assistance systems. Beyond driving, the design of automatic systems on the basis of a cybernetic model that represents actual cognitive, perceptual and motor processes may be relevant to human-machine interaction in different contexts.

Acknowledgements

The authors would like to thank all their collaborators on the various aspects of the work presented in this paper (in alphabetical order): Ablamvi Ameyoe, Fabien Claveau, Hervé Illy, Jean-François Lafay, Eric Le Carpentier, Louay Saleh and Chouki Sentouh.

Appendix. Detailed notations

A. Cybernetic driver model

- parameters: $\theta = [K_p \ K_c \ T_1 \ \tau_p \ K_r \ K_t \ T_n]$: see Table 1
- input and output signals: $u = [\theta_{far} \ \theta_{near} \ \delta_d \ \Gamma_s]^T$ and $y = [\hat{\Gamma}_d \ \hat{\delta}_{sw}]^T$
 - o θ_{near} angular deviation at a near point (θ_{near}) and θ_{far} at the tangent point, (see Fig. 1)
 - o δ_d steering wheel angle
 - o Γ_s steering wheel force feedback (see also vehicle model)
 - o $\hat{\Gamma}_d$: driver torque predicted/estimated by the model (Γ_d : real driver torque.)
 - o $\hat{\delta}_{sw}$ driver's intention in terms of steering wheel angle
- Δu , $\Delta \theta$, Δy : distraction signal assumed to be respectively input, parametric, or output disturbances; in this context, u_r , y_r are the disturbed input and output of the driver model (see Fig. 3); in order to simplify the notations, Δu and Δy may designate a perturbation on a part of the signal input (e.g. visual compensation signal in Fig. 6) or output signals ($\hat{\Gamma}_d$).
- state vector: $x_d = [x_{d1} \ x_{d2} \ x_{d3}]^T$

B. Distraction and haptic shared control (HSC) indicators and variables

- SDLP: standard deviation of lateral position
- SWRR: Steering wheel reversal rate
- LDR: Lane Departure Risk
- TLC: Time to Lane Crossing
- TLCP: Time to Lane Crossing - Path, i.e. TLC estimated by assuming that the vehicle yaw rate and heading speed were maintained as constant in the near future
- TPI: Torque prediction indicator
- IDI: Input default indicator
- $\Delta\delta$: driver error (deviation of the actual driver steering angle from that one predicted by the model)
- z: performance vector for HSC synthesis
- Γ_a, Γ_d : assistance and driver torque (applied on the steering wheel)
- Tco, Tres, Tcont: cooperation indicators for HSC systems (see Section 4.1)
- c_1, c_5, c_{da} : weights on signals that constitute the performance vector;

- c_1 : penalty for heading error
- c_2 : penalty for lateral deviation from the road centerline
- c_3 : penalty for the difference between the vehicle lateral acceleration and the expected lateral acceleration according to road curvature
- c_4 : penalty for the level of shared control
- c_5 : penalty for driver torque
- c_{da} : penalty for contradictory action between the driver and the automation. When $c_{da} < 0$, the minimization of the quadratic criteria is performed to avoid contradiction between the driver torque and the automation torque.

Relationship between the performance vector and the DVR model state and input:

$$\begin{bmatrix} \psi_L \\ y_{act} \\ a \\ \Gamma_a - \alpha \Gamma_d \\ \Gamma_d \\ \Gamma_a \end{bmatrix} = \begin{bmatrix} 0 & 0 & 1 & 0 & 0 & 0 & 0 & 0 & 0 & 0 \\ 0 & 0 & -l_s & 1 & 0 & 0 & 0 & 0 & 0 & 0 \\ V_x a_{11c} & V_x a_{12c} & 0 & 0 & V_x a_{15c} & 0 & 0 & 0 & 0 & 0 \\ 0 & 0 & 0 & 0 & 0 & 0 & 0 & 0 & -\alpha & 1 \\ 0 & 0 & 0 & 0 & 0 & 0 & 0 & 0 & 0 & 0 \\ 0 & 0 & 0 & 0 & 0 & 0 & 0 & 0 & 0 & 0 \end{bmatrix} \begin{bmatrix} \beta \\ r \\ \psi_L \\ y_L \\ \delta_d \\ \dot{\delta}_d \\ \delta_d \\ x_{1d} \\ x_{2d} \\ \Gamma_d \end{bmatrix} + \begin{bmatrix} 0 \\ 0 \\ 0 \\ 1 \\ 0 \\ 1 \end{bmatrix} \Gamma_a \quad (9)$$

C. Vehicle-road model (VR)

The general vehicle-road (VR) model considered for lateral control involves the dynamics of the lane keeping visual process, the steering column, and the lateral vehicle dynamics. According to Saleh, Chevrel and Lafay (2012), The VR model can be written as:

$$\dot{x}_{VR} = A_{VR} x_{VR} + B_{1VR} (\Gamma_a + \Gamma_d) + B_{2VR} \rho_{ref} \quad (10)$$

$A_{VR} \in \mathbb{R}^{6 \times 6}, B_{1VR} \in \mathbb{R}^{6 \times 1}, B_{2VR} \in \mathbb{R}^{6 \times 1}$

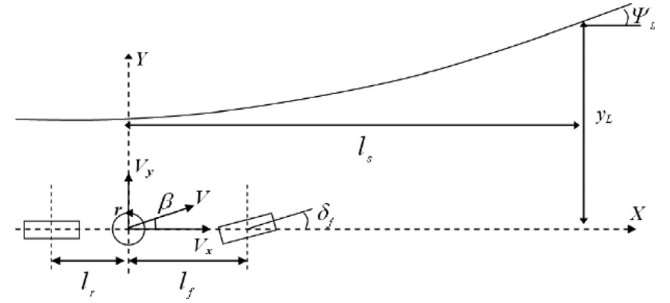


Fig. 10. Vehicle-road model for lane keeping.

Table 3 Peugeot 307 model parameters.

Parameter	Description	Value
l_f	Distance from Gravity Center to front axle	1.127 m
l_r	Distance from Gravity Center to rear axle	1.485 m
M	Total mass	1476 Kg
J	Vehicle yaw moment of inertia	1810 Kg m ²
C_{f0}	Front cornering stiffness	65,000 N/rad
C_{r0}	Rear cornering stiffness	57,000 N/rad
η_t	Tire length contact	0.185 m
μ	Adhesion	0.8
K_m	Manual steering column coefficient	1
R_s	Steering gear ratio	16
B_s	Steering system damping coefficient	5.73
I_s	Inertial moment of steering system	0.05 Kg m ²
l_s	Look-ahead distance	5 m

Where $x_{VR} = [\beta, r, \psi_L, y_L, \delta_d, d\delta_d/dt]^T$ is the VR state vector. It consists of (see Fig. 10): the side slip angle (β), the yaw rate (r), the heading angle (ψ_L), the offset from the lane centre (y_L) projected forward on the look-ahead distance (l_s), steering angle (δ_d) and steering speed ($d\delta_d/dt$).

The inputs of (2) are the steering torque command ($\Gamma_a + \Gamma_d$) and the road curvature (ρ_{ref}). The matrices A_{VR} , B_{1VR} and B_{2VR} are given by:

$$A_{VR} = \begin{pmatrix} a_{11c} & a_{12c} & 0 & 0 & a_{15c} & 0 \\ a_{21c} & a_{22c} & 0 & 0 & a_{25c} & 0 \\ 0 & 1 & 0 & 0 & 0 & 0 \\ V_x & l_s & V_x & 0 & 0 & 0 \\ 0 & 0 & 0 & 0 & 0 & 1 \\ a_{61c} & a_{62c} & 0 & 0 & a_{65c} & a_{66c} \end{pmatrix}, B_{1VR} = \begin{pmatrix} 0 \\ 0 \\ 0 \\ 0 \\ 0 \\ b_{61c} \end{pmatrix}, B_{2VR} = \begin{pmatrix} 0 \\ 0 \\ -V_x \\ -V_x l_s \\ 0 \\ 0 \end{pmatrix} \quad (11)$$

With:

$$\begin{aligned} a_{11c} &= -\frac{2(C_f + C_r)}{MV_x}, & a_{12c} &= \frac{2(C_r l_r - C_f l_f)}{MV_x^2} - 1, & a_{15c} &= \frac{2C_f}{MV_x R_s} \\ a_{21c} &= \frac{2(C_r l_r - C_f l_f)}{J}, & a_{22c} &= -\frac{2(C_f l_f^2 + C_r l_r^2)}{J V_x}, & a_{25c} &= \frac{2C_f l_f}{J R_s} \\ a_{61c} &= \frac{T_s \beta}{I_s}, & a_{62c} &= \frac{T_{Sr}}{I_s}, & a_{65c} &= -\frac{T_s \beta}{R_s I_s}, & a_{66c} &= -\frac{B_s}{I_s}, & C_r &= C_{r0} \mu \\ C_f &= C_{f0} \mu, & b_{61c} &= \frac{1}{I_s}, & T_s \beta &= \frac{2K_p C_f \eta_t}{R_s}, & T_{Sr} &= \frac{2K_p C_f \eta_t}{R_s} \frac{l_f}{V_x} \\ b_{12d} &= \frac{1}{T_l}, & a_{11d} &= -\frac{1}{T_l}, & b_{22d} &= -\frac{K_c}{V_x} \frac{2}{\tau_p} \frac{T_l}{T_l}, & a_{21d} &= \frac{K_c}{V_x} \frac{2}{\tau_p} \left(\frac{T_l}{T_l} - 1 \right) \\ a_{22d} &= -\frac{2}{\tau_p}, & b_{n31d} &= -b_{34d} T_{S\beta}, & b_{n32d} &= -b_{34d} T_{S\beta} \frac{l_f}{V_x}, & a_{33d} &= -\frac{1}{T_N} \end{aligned}$$

$$b_{32d} = \frac{K_r V_x + K_t}{T_N} \frac{K_c}{V_x} \frac{T_L}{T_I}, \quad b_{n35d} = b_{33d} + \frac{T_{SB}}{R_S} b_{34d}, \quad b_{34d} = -\frac{1}{T_N}$$

$$a_{32d} = 2 \frac{K_r V_x + K_t}{T_N}, \quad a_{31d} = -\frac{K_r V_x + K_t}{T_N} \frac{K_c}{V_x} \left(\frac{T_L}{T_I} - 1 \right),$$

$$b_{31d} = -K_p \frac{K_r V_x + K_t}{T_N}, \quad b_{33d} = -\frac{K_t}{T_N}, \quad b_{21d} = \frac{2}{\tau_p} K_p$$

VR parameters are summarized in Table 3 with nominal values that correspond to a Peugeot 307. This vehicle model was used on the driving simulator and supported shared lateral control synthesis.

References

- Abbink, D. A., Mulder, M., & Boer, E. R. (2012). Haptic shared control: Smoothly shifting control authority? *Cognition Technology & Work*, 14(1), 19–28. <https://doi.org/10.1007/s10111-011-0192-5>.
- Ameyoe, A. (2016). Estimation de la distraction fondée sur un modèle dynamique de conducteur: Principes et algorithmes (phdthesis). Ecole des Mines de Nantes, (October 6). Retrieved from <https://tel.archives-ouvertes.fr/tel-01395282/document>.
- Ameyoe, A., Chevrel, P., Le Carpentier, E., Mars, F., & Illy, H. (2015). Identification of a linear parameter varying driver model for the detection of distraction. *IFAC-PapersOnLine*, 48(26), 37–42. <https://doi.org/10.1016/j.ifacol.2015.11.110>.
- Ameyoe, A., Illy, H., Chevrel, P., Le Carpentier, E., & Mars, F. August 25, 2016. Retrieved from https://worldwide.espacenet.com/publicationDetails/biblio?FT=D&date=20160825&DB=&locale=en_EP&CC=WO&NR=2016132032A1&KC=A1&ND=4.
- Ameyoe, A., Mars, F., Chevrel, P., Le Carpentier, E., & Illy, H. (2015). Estimation of driver distraction using the prediction error of a cybernetic driver model. In *Proceedings of the driving simulation conference Europe 2015* (pp. 13–18). Tübingen.
- Cacciabue, P. C. (2007). *Modelling driver behaviour in automotive environments: critical issues in driver interactions with intelligent transport systems*. London: Springer.
- Donges, E. (1978). 2-level model of driver steering behavior. *Human Factors*, 20(6), 691–707.
- Dong, Y., Hu, Z., Uchimura, K., & Murayama, N. (2011). Driver inattention monitoring system for intelligent vehicles: A review. *IEEE Transactions on Intelligent Transportation Systems*, 12(2), 596–614. <https://doi.org/10.1109/TITS.2010.2092770>.
- Friszen, I., & Mars, F. (2014). The effect of visual degradation on anticipatory and compensatory steering control. *The Quarterly Journal of Experimental Psychology*, 67(3), 499–507. <https://doi.org/10.1080/17470218.2013.819518>.
- Godthelp, H., Milgram, P., & Blaauw, G. (1984). The development of a time-related measure to describe driving strategy. *Human Factors*, 26(3), 257–268.
- Hermannstädter, P., & Yang, B. (2013). Driver distraction assessment using driver modeling. In *2013 IEEE international conference on systems, man, and cybernetics* (pp. 3693–3698). <https://doi.org/10.1109/SMC.2013.629>.
- Hess, R. A., & Modjtahedzadeh, A. (1990). A control theoretic model of driver steering behavior. *IEEE Control Systems Magazine*, 10(5), 3–8. <https://doi.org/10.1109/37.60415>.
- Hoult, W., & Cole, D. J. (2008). A neuromuscular model featuring co-activation for use in driver simulation. *Vehicle System Dynamics*, 46, 175–189. <https://doi.org/10.1080/00423110801935798>.
- Illy, H., Ameyoe, A., Chevrel, P., Mars, F., & Le Carpentier, E. February 23, 2017. Retrieved from https://worldwide.espacenet.com/publicationDetails/biblio?FT=D&date=20170223&DB=&locale=en_EP&CC=WO&NR=2017029443A1&KC=A1&ND=4.
- Land, M. F., & Horwood, J. (1995). Which parts of the road guide steering. *Nature*, 377(6547), 339–340. <https://doi.org/10.1038/377339a0>.
- Land, M. F., & Lee, D. N. (1994). Where we look when we steer. *Nature*, 369(6483), 742–744. <https://doi.org/10.1038/369742a0>.
- Ljung, L. (1999). *System identification: theory for the user* (2 ed.). Upper Saddle River, NJ: Prentice Hall.
- Mammar, S., Glaser, S., & Netto, M. (2006). Time to line crossing for lane departure avoidance: A theoretical study and an experimental setting. *IEEE Transactions on Intelligent Transportation Systems*, 7(2), 226–241. <https://doi.org/10.1109/TITS.2006.874707>.
- Marro, G., & Zattoni, E. (2005). H2-optimal rejection with preview in the continuous-time domain. *Automatica*, 41(5), 815–821. <https://doi.org/10.1016/j.automatica.2004.11.030>.
- Mars, F. (2008). Driving around bends with manipulated eye-steering coordination. *Journal of Vision*, 8(11). <https://doi.org/10.1167/8.11.10>.
- Mars, F., Ameyoe, A., Chevrel, P., Carpentier, E. L., & Illy, H. (2017). Analysis of a driver model sensitivity to various types of distraction. Presented at the 5th international conference on driver distraction and inattention. Retrieved from: <https://hal.archives-ouvertes.fr/hal-01492034>.
- Mars, F., Deroo, M., & Charron, C. (2014). Driver adaptation to haptic shared control of the steering wheel. In *Proceedings of the 2014 IEEE international conference on systems, man, and cybernetics* (pp. 1524–1528). San Diego.
- Mars, F., Deroo, M., & Hoc, J.-M. (2014). Analysis of human-machine cooperation when driving with different degrees of haptic shared control. *IEEE Transactions on Haptics*, 7(3), 324–333. <https://doi.org/10.1109/TOH.2013.2295095>.
- Mars, F., & Navarro, J. (2012). Where we look when we drive with or without active steering wheel control. *Plos One*, 7(8), e43858. <https://doi.org/10.1371/journal.pone.0043858>.
- Mars, F., Saleh, L., Chevrel, P., Claveau, F., & Lafay, J.-F. (2011). Modeling the visual and motor control of steering with an eye to shared-control automation. In *Proceedings of the human factors and ergonomics society annual meeting: 55* (pp. 1422–1426). <https://doi.org/10.1177/1071181311551296>.
- Mulder, M., Abbink, D. A., & Boer, E. R. (2012). Sharing control with haptics: Seamless driver support from manual to automatic control. *Human Factors*, 54(5), 786–798.
- Mulder, M., Paassen, M. M. v., & Boer, E. R. (2004). Exploring the roles of information in the manual control of vehicular locomotion: from kinematics and dynamics to cybernetics. *Presence*, 13(5), 535–548. <https://doi.org/10.1162/1054746042545256>.
- Nakayama, O., Futami, T., Nakamura, T., & Boer, E. R. (1999). Development of a steering entropy method for evaluating driver workload. *SAE Transactions*, 108(6), 1686–1695.
- Plöchl, M., & Edelmann, J. (2007). Driver models in automobile dynamics application. *Vehicle System Dynamics*, 45(7–8), 699–741. <https://doi.org/10.1080/00423110701432482>.
- Saleh, L., Chevrel, P., Claveau, F., Lafay, J.-F., & Mars, F. (2012). Contrôle latéral partagé d'un véhicule automobile: Conception à base d'un modèle cybernétique du conducteur et d'une commande H2 anticipative. *Journal Européen Des Systèmes Automatisés*, 46(4–5), 535–557.
- Saleh, L., Chevrel, P., Claveau, F., Lafay, J.-F., & Mars, F. (2013). Shared steering control between a driver and an automation: stability in the presence of driver behavior uncertainty. *IEEE Transactions on Intelligent Transportation Systems*, 14(2), 974–983. <https://doi.org/10.1109/TITS.2013.2248363>.
- Saleh, L., Chevrel, P., & Lafay, J.-F. (2012). Optimal control with preview for lateral steering of a passenger car: Design and test on a driving simulator. In R. Sipahi, T. Vyhliđal, S.-I. Niculescu, & P. Pepe (Eds.), *Time delay systems: Methods, applications and new trends* (pp. 173–185). Berlin/Heidelberg: Springer. Retrieved from: http://link.springer.com/chapter/10.1007/978-3-642-25221-1_13.
- Saleh, L., Chevrel, P., Mars, F., Lafay, J.-F., & Claveau, F. (2011). Human-like cybernetic driver model for lane keeping. In S. Bittanti, A. Cenedese, & S. Zampieri (Eds.), *Proceedings of the 18th IFAC world congress* (pp. 4368–4373).
- Salvucci, D. D., & Gray, R. (2004). A two-point visual control model of steering. *Perception*, 33(10), 1233–1248. <https://doi.org/10.1068/p5343>.
- Sentouh, C., Chevrel, P., Mars, F., & Claveau, F. (2009). A sensorimotor driver model for steering control. In *Proceedings of the 2009 IEEE international conference on systems, man and cybernetics* (pp. 2462–2467).
- Sentouh, C., Soualmi, B., Popieul, J. C., & Debernard, S. (2013). Cooperative steering assist control system. In *2013 IEEE international conference on systems, man, and cybernetics* (pp. 941–946). <https://doi.org/10.1109/SMC.2013.165>.
- Summala, H., Nieminen, T., & Punto, M. (1996). Maintaining lane position with peripheral vision during in-vehicle tasks. *Human Factors*, 38(3), 442–451. <https://doi.org/10.1518/001872096778701944>.
- Wang, Z., Zheng, R., Kaizuka, T., Shimono, K., & Nakano, K. (2017). The effect of a haptic guidance steering system on fatigue-related driver behavior. *IEEE Transactions on Human-Machine Systems*, 1–8. PP(99) <https://doi.org/10.1109/THMS.2017.2693230>.
- Wilkie, R. M., Kountouriotis, G. K., Merat, N., & Wann, J. P. (2010). Using vision to control locomotion: Looking where you want to go. *Experimental Brain Research*, 204(4), 539–547. <https://doi.org/10.1007/s00221-010-2321-4>.
- Yang, Y., McDonald, M., & Zheng, P. (2012). Can drivers' eye movements be used to monitor their performance? A case study. *IET Intelligent Transport Systems*, 6(4), 444–452. <https://doi.org/10.1049/iet-its.2012.0008>.